

Improving the Interfacial Stability of Ultrahigh-Nickel Cathode with PEO-based Electrolyte by Targeted Chemical Reactions

Yuqing Dai,^a Zihan Hou,^a Gui Luo,^b Duo Deng,^b Wenjie Peng,^{a,b,c} Zhixing Wang,^{a,c} Huajun Guo,^{a,c} Xinhai Li,^{a,c} Guochun Yan,^{a,c} Hui Duan,^{a,c} Wenchao Zhang^{a,c} and Jiexi Wang*^{a,c}

[a] Engineering Research Center of the Ministry of Education for Advanced Battery Materials, Hunan Provincial Key Laboratory of Nonferrous Value-Added Metallurgy, School of Metallurgy and Environment, Central South University, Changsha 410083, China. E-mail: wangjiexikeen@csu.edu.cn

[b] BASF ShanShan Battery Material Co., LTD, Changsha 410205, China.

[c] National Engineering Research Centre of Advanced Energy Storage Materials, changsha 410205, China

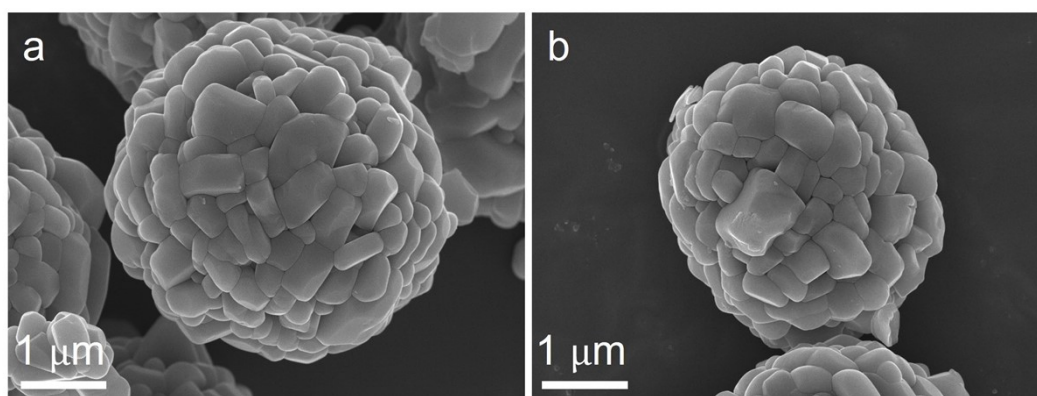


Fig. S1. SEM images of (a) LBO2-NCM and (b) LBO3-NCM.

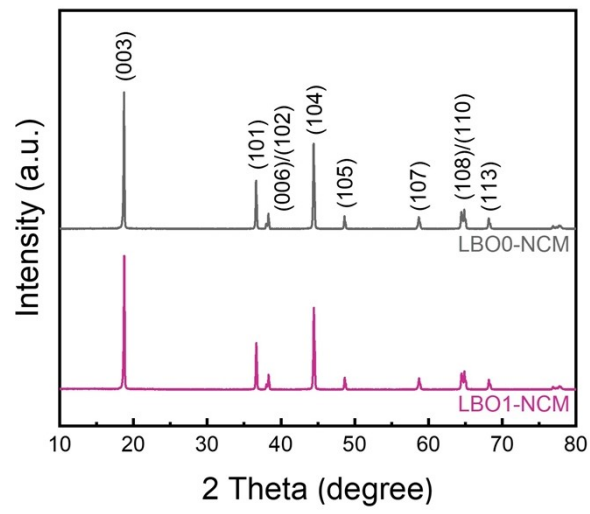


Fig. S2. XRD patterns of LBO0-NCM and LBO1-NCM.

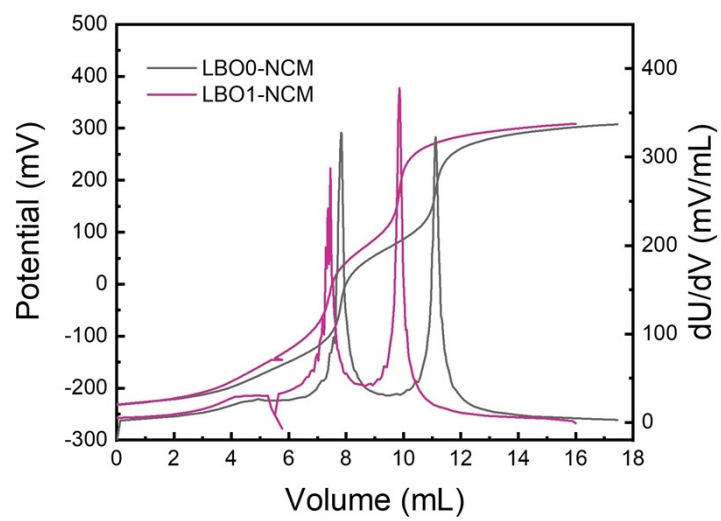


Fig. S3. Electrometric titration curve of LBO0-NCM and LBO1-NCM.

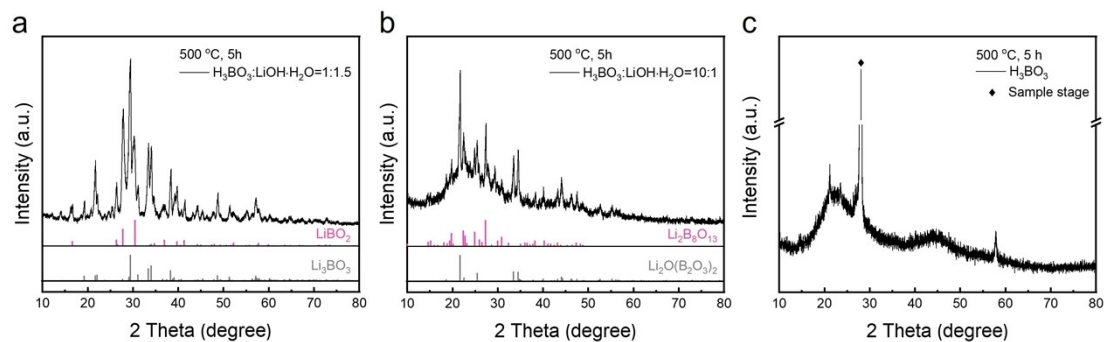


Fig. S4. XRD patterns of samples sintered with different mole ratio of H_3BO_3 and $\text{LiOH} \cdot \text{H}_2\text{O}$.

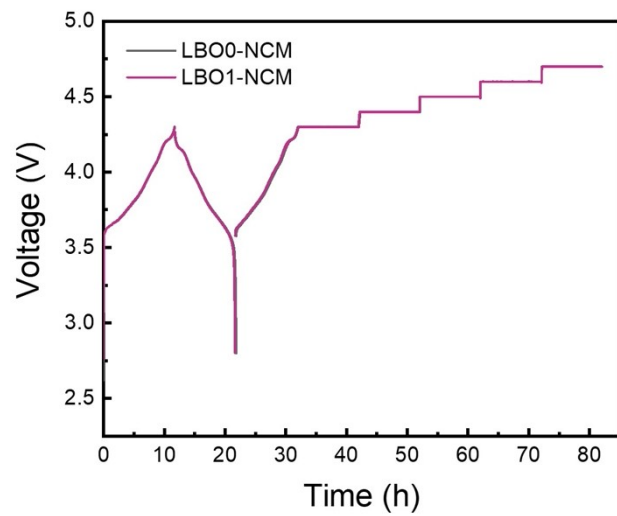


Fig. S5. The voltage curve of the three-electrode PEO-based SLMB during the measuring procedure of this study.

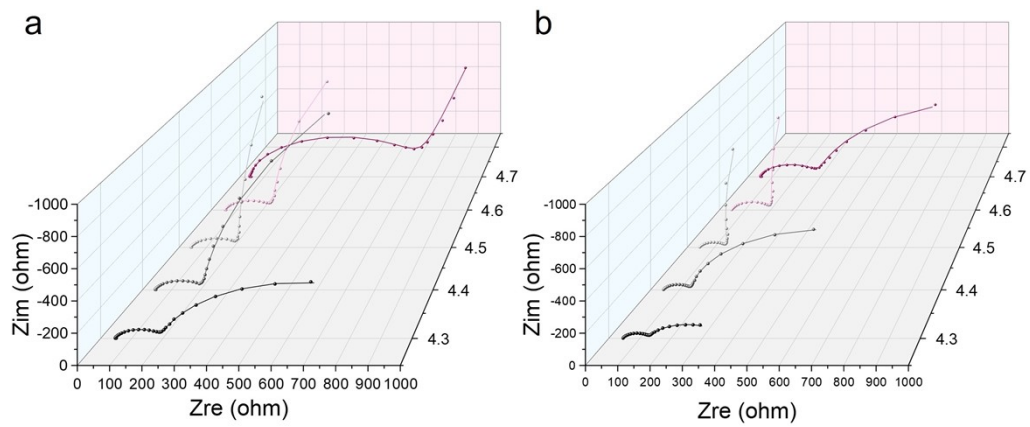


Fig. S6. The Nyquist plots of the three-electrode (a) Li|PEO|LBO0-NCM and (b) Li|PEO|LBO1-NCM.

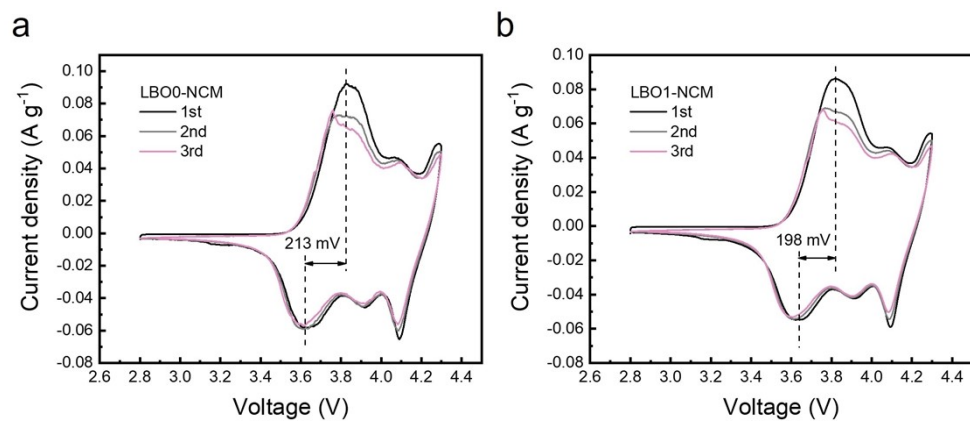


Fig. S7. CV curves of the pristine (a) LBO0-NCM and (b) LBO1-NCM in the first three consecutive cycles between 2.8-4.3 V with a scanning rate of 0.05 mV s⁻¹.

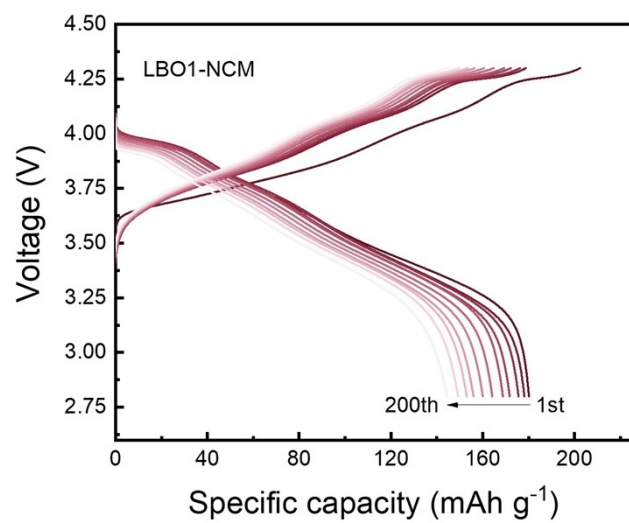


Fig. S8. Corresponding charge/discharge curves of Li|PEO|LBO1-NCM pouch cell at different electrochemical cycles.

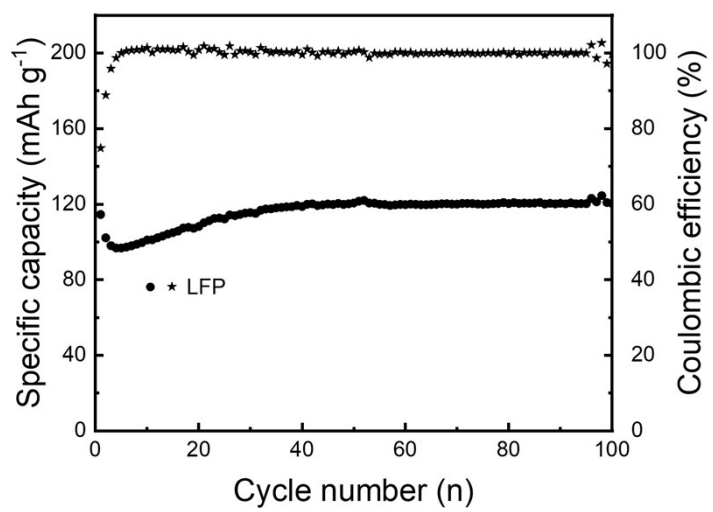


Fig. S9. Cycling performance and the corresponding Coulombic efficiency at 0.5C of Li|PEO|LFP.

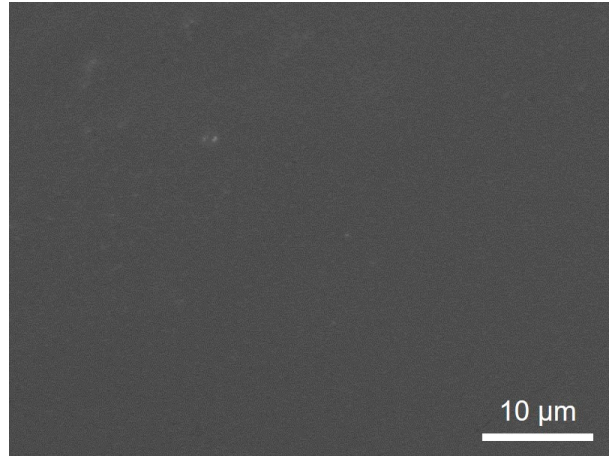


Fig. S10. The SEM images of the disassembled-lithium metal after 100 cycles in Li|PEO|LFP.